Available online at www.sciencedirect.com
ScienceDirect
Journal of Power Sources 176 (2008) 200–206
JOURNAL OF POWER SOURCES
www.elsevier.com/locate/jpowsour

Modeling of gas transport through a tubular solid oxide fuel cell and the porous anode layer

John R. Izzo Jr., Aldo A. Peracchio, Wilson K.S. Chiu *

Department of Mechanical Engineering, University of Connecticut, 191 Auditorium Road, Storrs, CT 06269-3139, United States

Received 9 September 2007; received in revised form 16 October 2007; accepted 16 October 2007
Available online 30 October 2007

Abstract

A design model is a necessary tool to understand the gas transport phenomena that occurs in a tubular solid oxide fuel cell (SOFC). This paper describes a computational model, which studies the gas flow through an anode-supported tubular SOFC and the subsequent diffusion of gas through its porous anode. The model is a numerical solution for the gas flow through a plug flow reactor with a diffusion layer, which includes the activation, ohmic, and concentration polarizations. Gas diffusion is modeled using the dusty-gas equations which include Knudsen diffusion. Mercury intrusion porosimetry (MIP) is used to experimentally determine micro-structural parameters such as porosity, tortuosity and effective diffusion coefficients, which are used in the diffusion equations for the porous anode layer. It was found that diffusion in the anode plays a key role in the performance of a tubular SOFC. The concentration gradient of hydrogen and water results in a lower concentration of hydrogen and a higher concentration of water at the reactive triple phase boundary (TPB) than in the fuel stream which both lead to a lower cell voltage. The gas diffusion determines the limiting current density of the cell where a higher concentration drop of hydrogen results in a lower limiting current density. The model validates well with experimental data and is used to improve micro-tubular solid oxide fuel cell designs.

Keywords: Tubular solid oxide fuel cell; Gas transport; Performance modeling; Mercury intrusion porosimetry

1. Introduction

Tubular solid oxide fuel cells (SOFCs) have become a promising choice for power generation and a detailed analysis is necessary to examine different operating conditions [1]. Gas transport is important to understand in order to increase the performance of the fuel cell. Micro-structural parameters largely affect the gas transport, which typically spans the continuum to free molecule regimes, and models reflecting the effects of these parameters on performance are being developed. Past works have modeled heat transfer, species transportation and electrochemical reaction effects in a collective manner with a control volume approach [2]. Some detailed diffusion models have used Fick's law [3–5] because the gas distribution in the anode can be analytically solved. Other works have extended the gas diffusion to include interactions between the molecules of the multicomponent gas by using the Stefan–Maxwell equations [6,7] but do not consider molecule–wall interactions in the pores with Knudsen diffusion. The dusty-gas model [8,9] is the most complete diffusion model which considers molecule–molecule and molecule–wall interactions in the porous media while allowing total concentration to vary through the anode and is applied in this work. A comparison between the different diffusion models, i.e. Fick's, Stefan–Maxwell and dusty-gas to predict the concentration polarization in a SOFC anode is presented elsewhere in Ref. [10]. Recent Modeling of a tubular SOFC considers heat transfer, species transportation, and electro-chemical reactions with activation, ohmic, and concentration polarizations. Such models are difficult to use and are quite complicated. Constant total concentration is typically assumed through the anode which is not valid for detailed diffusion in the non-continuum regime. Current models also lack actual pore property measurements and often rely on empirical data or tuning parameters.

In the current work, mercury intrusion porosimetry (MIP) is used to experimentally measure the pore size distribution in the porous anode layer. Results are used to determine bulk micro-structure properties, which are then included in a simple, computationally inexpensive 1D plug flow reactor (PFR)

* Corresponding author. Tel.: +1 860 486 3647; fax: +1 860 486 5088.
E-mail address: wchiu@engr.uconn.edu (W.K.S. Chiu).

0378-7753/$ – see front matter © 2007 Elsevier B.V. All rights reserved.
doi:10.1016/j.jpowsour.2007.10.075

Nomenclature

A	area
C_i	concentration of species i
C_T	total concentration of all species
D	pore diameter
D_{eff}	mean hydraulic diameter
$\tilde{D}_{ij}$	binary diffusion coefficient of species i in species j
$\tilde{D}_i^k$	Knudsen diffusion coefficient for species i
D_{ij}	effective binary diffusion coefficient of species i in species j
D_i^k	effective Knudsen diffusion coefficient for species i
E	Nernst voltage
E_{op}	operating voltage
F	Faradays constant
F_T	total inlet flow rate
$\Delta\bar{g}_f$	change in Gibb's free energy
i	current density
$i_{0,a/c}$	exchange current density for anode and cathode
n	number of electrons involved in reaction
N_i	molar flux of species i
N_T	total molar flux of all species
p_i	partial pressure of species i
P	perimeter
r	area specific resistance
R	universal gas constant
$\Re_j$	reaction rate of hydrogen and oxygen ion reaction
S	effective diffusion area to total area ratio
T	temperature
V_{void}	pore volume
V_T	total volume
x_i	molar fraction of species i
x	distance through anode

Greek

α_n	normalized rate of infusion of mercury
β	transfer coefficient
γ	surface tension
ε	porosity
η_{Act}	activation polarization
η_{Conc}	concentration polarization
η_{Ohm}	ohmic polarization
θ	contact angle
τ	tortuosity

Subscripts

a	anode
c	cathode
Act	activation
Conc	concentration
Ohm	ohmic
void	pore or void space
i	species i
T	total
j	species j
sup	supply channel
op	operating

tubular SOFC model to predict the polarization of the fuel cell. The advantage to the proposed model is its simplicity and low computational cost while still capturing the important polarization and diffusion physics needed to accurately predict the performance of an SOFC. Diffusion in the anode is modeled with the dusty-gas equations for three species, which allows the total concentration to vary due to Knudsen diffusion, and are integrated in closed form. The diffusion equations predict concentration levels through the porous anode and at the reactive TPB. Polarization losses are then calculated and cell performance is predicted. The model is validated against test data and used to study structural parameters and conditions for optimal SOFC performance.

2. Methods of approach

2.1. Mercury intrusion porosimetry

In order to accurately model gas diffusion through the porous anode, it is necessary to determine the porosity and tortuosity (pore effective length/actual length) of the material. MIP data can be used to generate a pore size distribution curve and to calculate the porosity and tortuosity. The anode samples (Adaptive Materials Inc., Ann Arbor, MI) studied are composed of nickel and yttria-stabilized zirconia (Ni-YSZ). Intruded mercury measurements are used directly with Eq. (1) to calculate the porosity, which is the ratio of the void volume to the total volume of the sample:

$$\varepsilon = \frac{V_{void}}{V_T} \tag{1}$$

The pressure required to intrude mercury into a pore is related to the pore diameter through the Washburn equation [11] given in Eq. (2), where γ and θ are the surface tension and contact angle of mercury, respectively.

$$D = -\frac{2\gamma\cos\theta}{P} \tag{2}$$

A normalized pore size distribution (the rate of change of infusion volume of mercury with respect to diameter normalized by the bulk volume) can be obtained by differentiating the cumulative volume versus pore diameter with respect to pore diameter and dividing by the total volume shown in Eq. (3). The pore size distribution is used to obtain the tortuosity and effective diffusion coefficients as discussed in the next section.

$$\alpha_n = \left(\frac{1}{V_T}\right)\frac{dV}{dD} \tag{3}$$

2.2. Tortuosity and effective area formulation using the pore size distribution function

In modeling the diffusion process in the fuel cell, an effective diffusion area and effective length for the diffusion through the fuel cell's porous media are needed. As described above, the MIP measurements provide the porosity the normalized pore size distribution as a function of diameter. Using this information, it is possible to develop equations for the effective diffusion area per total area, S, and tortuosity, τ. The equations assume an average value for tortuosity, independent of pore size. The porosity can also be calculated from the normalized pore size distribution as

$$\varepsilon = \int \alpha_n \, \mathrm{d}D \tag{4}$$

The effective diffusion area to total area ratio is related to the porosity and tortuosity.

$$S = \frac{\varepsilon}{\tau} \tag{5}$$

The equation for tortuosity is developed by modeling the flow through the pores (accounting for the varying pore diameters using α_n) and the equation for friction in a pipe with laminar flow. Laminar flow is assumed in each pore with each pore ascribed an effective length in terms of tortuosity to determine the pressure drop across the pore in terms of the unknown tortuosity. Adding the Ergun equation [12], relating pressure drop through a porous media to a Reynolds number based on porous media particle size allows for the solution of tortuosity.

$$\tau^2 = \frac{2.083}{(D_{\mathrm{eff}})^2 \varepsilon} \int D^2 \alpha_n \, \mathrm{d}D \tag{6}$$

where $D_{\mathrm{eff}} = \varepsilon/(\int (1/D)\alpha_n \mathrm{d}D)$. The multi-component dusty-gas diffusion equations used span the free molecule to continuum regimes. Accordingly, effective Knudsen and binary continuum diffusion coefficients are required to account for the diffusion through the porous anode material. The binary continuum diffusion coefficients are corrected using the following equation:

$$D_{ij} = \frac{\varepsilon}{\tau} \tilde{D}_{ij} \tag{7}$$

The effective Knudsen diffusion coefficients depend on pore diameter, and are therefore averaged over the pore diameter variation of the anode material.

$$D_i^k = \frac{1}{\tau} \int \tilde{D}_i^k \alpha_n \, \mathrm{d}D \tag{8}$$

2.3. Model assumptions and boundary conditions

The model treats the three component gas (hydrogen, water, inert) flow in the tubular SOFC as an axially segmented plug-flow reactor (PFR), where the gas velocity profile is uniform and all equations are steady state. The model is assumed to be isothermal. The current density is assumed to be uniformly distributed along the length of the tube and constant. The TPB is treated as a reactive boundary at the edge of the anode where it comes into contact with the electrolyte. Chan and Xia [13] have studied the concentration polarization for each electrode in an anode-supported SOFC and have reported negligible loss in the cathode. Zhu and Kee [14] have also reported negligible cathode concentration polarization in an anode-supported SOFC. Therefore, mass transfer effects in the cathode is assumed negligible because an anode-supported SOFC is composed of a cathode that is much thinner than the anode, resulting in small concentration losses. The model is capable of predicting mass transport in the supply channel and anode diffusion layer, Nernst voltage distribution along the tube, polarization losses, the onset of limiting current density, and the polarization curve of the fuel cell.

The species flux required to run the fuel cell at the specified constant current density is based on a faradaic relationship and depends on the reaction rate of the electro-chemical reaction with hydrogen and oxygen ions at the TPB. The species flux occurs at the TPB and since there is no generation in the anode, the flux is constant throughout the anode. At the anode–supply channel interface, a species flux is prescribed based on species diffusion through the anode and current draw at the TPB. Since hydrogen and water are the only species used in the electro-chemical oxidation reaction, the flux of inert gas into the TPB is zero and with a mole balance the flux of water is equal and opposite the flux of hydrogen. Therefore the species flux equations for each axial segment of the PFR are first order ordinary differential equations because the species flux into the anode is a constant for a given current density. These equations require initial species flux values at the inlet to the fuel cell, i.e.

$$N = N_{i,0} \quad \text{at the inlet} \tag{9}$$

The flux through the anode of each species is used in the dusty-gas diffusion equations to specify the concentration gradient through the anode. The equations are first-order and therefore only require initial concentration values for each species.

$$C = C_{i,0} \quad \text{at the start of anode layer} \tag{10}$$

The model input parameters include the initial conditions described above, physical dimensions, operating conditions, polarization and diffusion parameters. The fuel cell length, inner diameter and layer thicknesses are required for the physical dimensions where the cross-sectional area and perimeter are calculated. The temperature, pressure, current density, and inlet species flow rates are required for the operating conditions. The change in Gibb's free energy, exchange current densities (both electrodes) and an overall cell resistance are required for the polarization parameters. The porosity, tortuosity, binary and Knudsen diffusion coefficients are required for the diffusion parameters. Any other required parameters are constants.

2.4. Governing equations

The rate of the electro-chemical reaction that consumes hydrogen to produce water and electrons at the TPB is related to the change in molar flux of species i along the length of the PFR, Eq. (11). The subscript $i = 1, 2, 3$ corresponds to hydrogen, water and inert gas species, respectively. The species flux is related to

the mole fraction of species i by Eq. (12):

$$\frac{dN_i}{dz} = \Re_j = \frac{P}{A}\left(\frac{i}{2F}\right) \tag{11}$$

$$x_i = \frac{C_i}{C_T} = \frac{N_i}{N_T} \tag{12}$$

The voltage along the TPB is calculated using the Nernst equation [15] which considers the partial pressure of the gases at the TPB, and is given in Eq. (13). The operating voltage, Eq. (14), is calculated with the Nernst voltage and the polarization losses described in the next section.

$$E = \frac{\Delta \bar{g}_f}{2F} + \frac{RT}{2F}\ln\left(\frac{p_{hydrogen}\, p_{oxygen}^{1/2}}{p_{water}}\right) \tag{13}$$

$$E_{op} = E - \eta_{Act} - \eta_{Ohm} \tag{14}$$

2.5. Polarization losses

Activation polarization in the SOFC for both electrodes (subscript a and c) can be expressed by the Butler–Volmer equation, where the transfer coefficient is usually prescribed as 0.5 for fuel cell applications [5]. The exchange current density is dependent on operating conditions such as temperature and pressure and the concentration of gas species at the TPB for each electrode [1] and is still an active area of research, however an appropriate constant value of 530 and 200 mA cm^{-2} were used in this study for the anode and cathode, respectively [5]:

$$i = i_{0,a/c}\left[\exp\left(\beta\frac{nF\eta_{Act,a/c}}{RT}\right) - \exp\left(-(1-\beta)\frac{nF\eta_{Act,a/c}}{RT}\right)\right] \tag{15}$$

The ohmic polarization occurs from the electronic resistance in the electrodes and the ionic resistance in the electrolyte. The polarization can be expressed with an area specific resistance value [5,14].

$$\eta_{Ohm} = ir \tag{16}$$

The concentration polarization occurs from a concentration gradient of the fuel as it diffuses through the porous anode layer to the TPB where the power producing chemical reactions occur. The polarization itself can be separately calculated by subtracting the Nernst voltage at the TPB from its value based on reactant supply channel (SC) conditions [14].

$$\eta_{Conc} = E_{sup} - E \tag{17}$$

2.6. Diffusion equations

The dusty-gas equations [17,18] are given below for a three component gas, where the water vapor flux is the negative of the hydrogen flux at the TPB and the inert flux is zero. An inert species is required to accurately model the diffusion process because it affects the diffusion in the anode even though it has zero flux from interactions with the water and hydrogen molecules. The viscous flux term in the dusty-gas equations was neglected due to an estimation of the term for this case that showed it was an order of magnitude smaller than the other terms. These equations govern the mass transfer in the anode layer where the subscripts 1, 2, 3 correspond to hydrogen, water, and inert gas species, respectively.

$$\frac{N_1}{D_1^k} + \frac{1}{D_{12}}(y_2N_1 - y_1N_2) + \frac{1}{D_{13}}(y_3N_1) = -\frac{dC_1}{dx} \tag{18}$$

$$\frac{N_2}{D_2^k} + \frac{1}{D_{21}}(y_1N_2 - y_2N_1) + \frac{1}{D_{23}}(y_3N_2) = -\frac{dC_2}{dx} \tag{19}$$

$$-\frac{1}{D_{31}}(y_3N_1) - \frac{1}{D_{32}}(y_3N_2) = -\frac{dC_3}{dx} \tag{20}$$

The dusty-gas equations are analytically integrated, resulting in the following equations for concentration as a function of distance through the anode. In this study, the total concentration depends on x, since this is the actual behavior, and is not assumed constant to simplify the problem.

$$C_1 = C_{10} - N_1xB_1 - C_{30}B_2[(1+ax)^{\mu} - 1] \tag{21}$$

$$C_2 = C_T - C_1 - C_3 \tag{22}$$

$$C_3 = C_{30}(1+ax)^{\mu} \tag{23}$$

$$C_T = C_{T0}(1+ax) \tag{24}$$

The constants used in the equations are as follows:

$$a = \left(\frac{N_1}{C_{T0}}\right)\left(\frac{1}{D_2^k} - \frac{1}{D_1^k}\right), \quad \mu = \frac{1/D_{13} - 1/D_{23}}{1/D_2^k - 1/D_1^k},$$

$$B_1 = \frac{1}{D_1^k} + \frac{1}{D_{12}}, \quad \text{and} \quad B_2 = \frac{1/D_{13} - 1/D_{12}}{1/D_{13} - 1/D_{23}}$$

2.7. Numerical method

The SOFC model was programmed and analyzed using Matlab. The differential species flux equations are solved with the built in ordinary differential equation solver (ode45) based on an explicit adaptive Runge–Kutta scheme. This is suitable for relaxation of the constant current density assumption where a numerical solution is required. The size of the control volumes in the tube were started coarse and made finer until grid independence was achieved. To further check the numerical model, the predicted voltage values matched a complete analytical solution of the flux equations in the fuel stream, showing they are in very good agreement and the numerical solution is accurate.

3. Results and discussion

3.1. Experimental validation of model

The numerical model was further validated against experimental data published in Refs. [2,19]. The experiment used a tubular solid oxide fuel cell very similar in size and material to the current study. The experimental conditions and structural parameters used for this simulation are from Refs. [2,20]. A pore

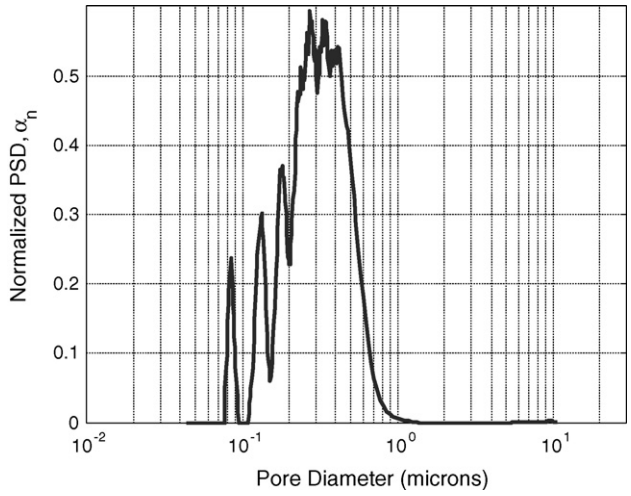

Fig. 1. Normalized pore size distribution curve. Most of the pores fall in the diameter range of 0.1 and 1 μm.

size distribution is needed to correct the diffusion coefficients and determine other structural parameters of the material. The pore size distribution for the studied material shown in Fig. 1 is used to adjust the diffusion coefficients, using Eqs. (7) and (8), because the porosity, tortuosity and material of the samples being studied are very similar to those reported [20]. Most of the pores in the studied material are between 0.1 and 1.0 μm, based on the experimental data in Fig. 1. The binary diffusion coefficients and the Knudsen diffusion coefficients are calculated from [16] and [17], respectively.

The numerical SOFC model predicts the polarization curve very well as shown in Fig. 2. In this validation, the lowest discrepancy of 3.3% error occurs at the open circuit voltage, while a maximum error of 8.7% occurs at high current densities.

3.2. Application of model

This study is performed to examine the variation in the gas concentration of the fuel and the operating voltage along the anode layer in a tubular SOFC. The test conditions are summarized in Table 1. The polarization curve is given in Fig. 3a and the limiting current density, where the hydrogen concentration at the TPB approaches zero by the end of the tubular SOFC, was calculated to be approximately 429.58 mA cm^{-2}. The fuel utilization in this case is 93.3%. The fuel is not fully utilized at the limiting current density because the hydrogen concentration is not approaching zero in the supply channel, rather it is approaching zero at the TPB after diffusion through the anode. The fuel cannot be fully utilized if there is any concentration drop through the anode. For the given anode properties and current densities, it is observed in Fig. 3 that the concentration polarization is small. This is the case at low operating current densities, but the concentration polarization does become significant at higher current densities. The polarization curve in Fig. 3 does not capture local variations because in the model the values are averaged over the tube in order to generate the polarization curve. It is necessary to model the diffusion process locally in the tube because there are significant variations in the local hydrogen concentration at the TPB and high local concentration polarizations arise. The local gas and operating voltage distributions along the SOFC tube at the supply channel (SC) and the triple phase boundary (TPB) are given in Figs. 3 and 4b respectively for an operating current density near the limiting current density of 429.5 mA cm^{-2}. The model is capable of pre-

Table 1
Model parameters used for gas and voltage variation study

Parameter	Symbol	Value
Fuel cell length (mm)	L	65
Fuel cell diameter (mm)	D	2.7
Hydrogen mole fraction	x_1	0.3491
Water mole fraction	x_2	0.2020
Inert mole fraction	x_3	0.4488
Total inlet flow rate (sccm)	F_T	189.8
Temperature (K)	T	1023
Pressure (atm)	P	1
Overall cell resistance (Ω)	r	0.16
Anode thickness (μm)	l_a	250
Porosity	ε	0.25
Tortuosity	τ	2

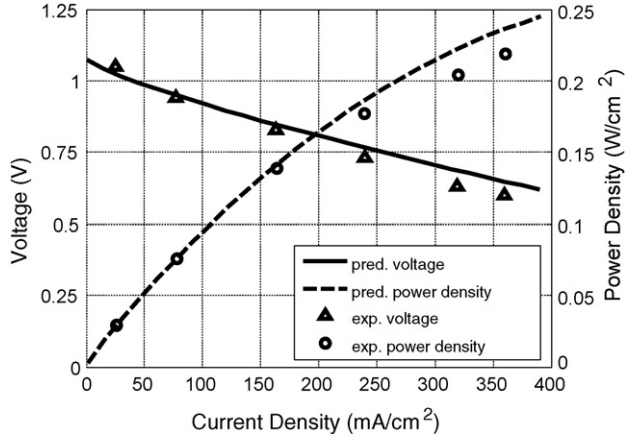

Fig. 2. Comparison of numerically predicted polarization and power density curves with experimental data [2].

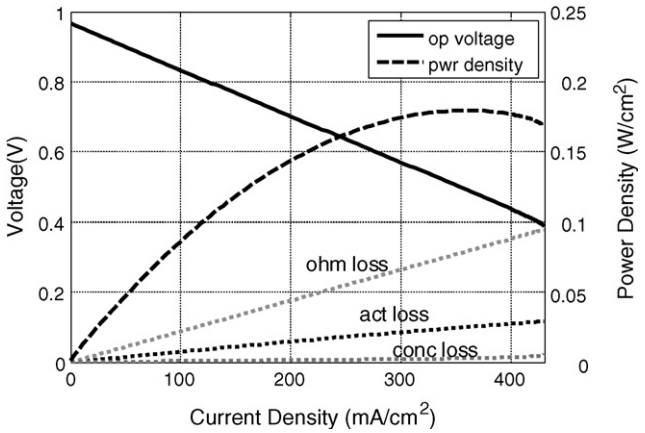

Fig. 3. The polarization curve, power density curve, and corresponding ohmic, activation and concentration losses in a tubular SOFC.

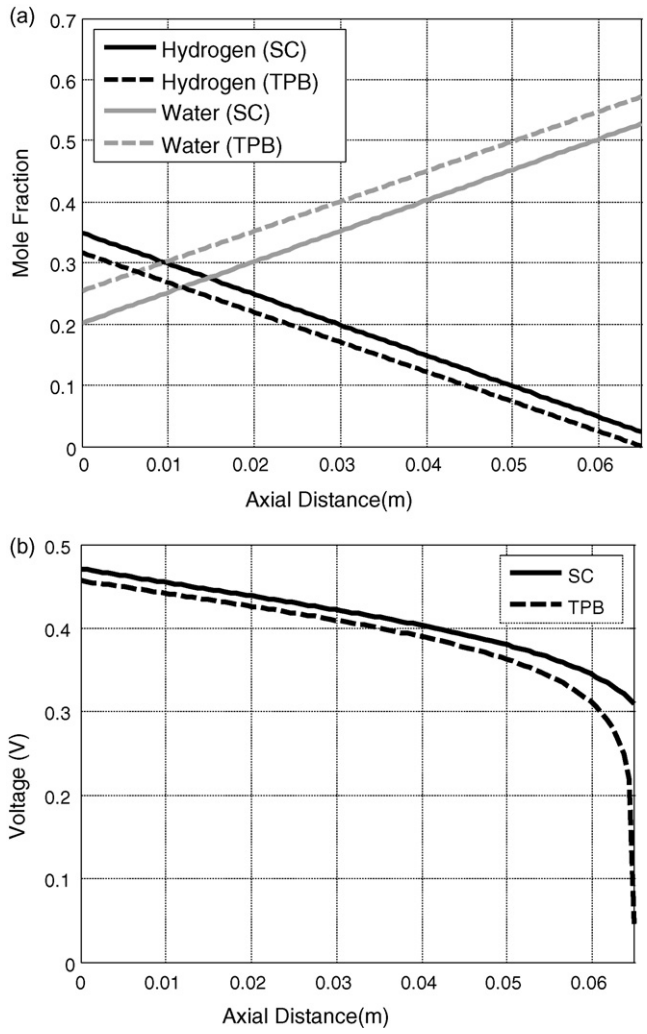

Fig. 4. Mole fraction of gases (a) and operational voltage (b) along the tubular SOFC considering only the supply channel (SC), and at the triple phase boundary (TPB) when the anode gas diffusion layer is included.

dicting the onset of the limiting current density, however a much more complex approach is required to predict the fuel cell characteristics of the limiting current process [21]. The reader can consider advanced reaction kinetics and mass transfer limitations in this operation regime. Gas species concentrations at the SC and TPB are the two bounding cases for SOFC performance in the diffusion model. The highest cell voltage occurs if the concentration of the gas species for the electro-chemical reaction experiences no drop and is equal to the concentrations in the SC. The lowest cell voltage occurs when there is a concentration gradient across the anode layer and the electro-chemical reaction takes place with the gas species concentrations after diffusion to the TPB.

The addition of the diffusive anode layer has an important effect on the mole fraction distribution of hydrogen and water and must be included for an accurate model. It is shown in Fig. 4a that the concentration of hydrogen and water vary considerably along the tubular SOFC as the power-producing electro-chemical reactions occur. Due to the addition of the anode layer, there is a concentration drop of hydrogen and an increase in concentration of water through the anode. This results in a higher concentration loss and a lower voltage in the fuel cell because the Nernst voltage decreases with a lower hydrogen concentration or a higher water concentration at the TPB. The change in hydrogen mole fraction drops by 0.0320 and 0.0234 at the start and end of the tube respectively while the change in water mole fraction increases by 0.0526 and 0.0440 at the start and end of the tube, respectively. The change in the water concentration is greater than the hydrogen change since the Knudsen diffusion term is different for both hydrogen and water. The concentration profiles in the anode are approximately linear and the slope is constant for a given current density. With an increase in current density, the flux across the anode becomes higher and the slope of the concentration profile changes. The higher flux results in a larger concentration change across the anode where there will be a higher concentration loss and a lower Nernst voltage. When the thickness of the anode layer is increased, the concentration gradient is the same because it is dependent on the current density but the overall difference in concentration is greater. This results in a higher concentration loss and a lower Nernst voltage. The limiting current density of the cell is lower because of the larger concentration drop of hydrogen so the fuel cell will become hydrogen starved at a lower current density. It would be ideal from a concentration polarization stand point to make the anode thin and highly porous to facilitate better gas diffusion, but the anode also functions as an electron carrier, catalyst and sometimes a support so there is a delicate balance between all of these.

The variation of gas concentration in the fuel cell leads to a non-uniform voltage distribution in the tube. The model takes the average voltage along the tube length for a given current density. The axial voltage distributions for the conditions given above are shown in Fig. 4b at an operating current density of 429.5 mA cm^{-2}. Once again the addition of the diffusive anode layer has a significant effect, this time on the voltage. The voltage drop is 0.0145 V at the start of the tube and 0.2633 V at the end of the tube. The largest loss comes at the end of the tube because we are approaching the limiting current density and the hydrogen concentration is approaching zero, as can be seen in the previously shown axial gas species distribution for this case in Fig. 4a. The voltage in the cell drops off because there is no fuel for the electro-chemical oxidation reaction at the TPB. The limiting current density is lower with a concentration drop of hydrogen at the TPB from diffusion across the anode. The voltage calculated with no diffusion layer (SC) does not start to decrease sharply at the current density run for the case presented in Fig. 4b because the hydrogen concentration does not approach zero. It is shown that the diffusion model is necessary to include in the analysis to accurately predict the SOFC performance and study local variations in hydrogen concentration and Nernst voltage.

4. Conclusions

The gas transport is critical in SOFC performance and can give large losses in a poorly designed system. This study examined the gas transport and polarization in an anode-supported

tubular SOFC. Critical parameters and properties, such as porosity and tortuosity, were obtained from MIP experiments in order to study a specific micro-structure. A numerical SOFC model with a diffusive anode layer, shown in this study to be critical for accuracy, was developed to predict the gas transport and cell performance. The model validated well with the experimental results as the error was between 3.3 and 8.7% in the voltage predictions. There is a significant variation in the gas and voltage distributions along the SOFC tube when the diffusive anode layer is included. It was observed that the hydrogen concentration drops and the water concentration increases at the TPB due to diffusion across the anode which resulted in a lower Nernst voltage of the cell. The voltage of the cell experiences a large drop when the hydrogen concentration at the TPB approaches zero, which results in high local concentration polarizations. It is necessary to include the diffusive anode layer in the numerical model to obtain accurate results and the design of the layer is critical to SOFC performance.

Acknowledgments

Financial support from the Army Research Office is gratefully acknowledged. SOFC anode samples were provided by Adaptive Materials Inc. (Ann Arbor, MI). Mercury porosimetry measurements were performed by Brandon Chalifoux.

References

[1] S. Campanari, P. Iora, J. Power Sources 132 (2004) 113–126.
[2] X. Xue, J. Tang, N. Sammes, Y. Du, J. Power Sources 142 (2005) 211–222.
[3] D. Sanchez, R. Chacartegui, A. Munoz, T. Sanchez, J. Power Sources 160 (2006) 1074–1087.
[4] J.R. Ferguson, J.M. Fiard, R. Herbin, J. Power Sources 58 (1996) 109–122.
[5] S.H. Chan, K.A. Khor, Z.T. Xia, J. Power Sources 93 (2001) 130–140.
[6] S. Nagata, A. Momma, T. Kato, Y. Kasuga, J. Power Sources 101 (2001) 60–71.
[7] M. Iwata, T. Hikosaka, M. Morita, T. Iwanari, K. Ito, K. Onda, Y. Esaki, Y. Sakaki, S. Nagata, Solid State Ionics 132 (2000) 297–308.
[8] Y. Shi, N. Cai, C. Li, J. Power Sources 164 (2007) 639–648.
[9] H. Zhu, R.J. Kee, J. Electrochem. Soc. 153 (2006) A1765–A1772.
[10] R. Suwanwarangkul, E. Croiset, M.W. Fowler, P.L. Douglas, E. Entchev, M.A. Douglas, J. Power Sources 122 (2003) 9–18.
[11] E.W. Washburn, Phys. Rev. 17 (1921) 273–283.
[12] M.M. Denn, Process Fluid Mechanics, Prentice-Hall Inc., New Jersey, 1980, pp. 67–71.
[13] S.H. Chan, Z.T. Xia, J. Appl. Electrochem. 32 (2002) 339–347.
[14] H. Zhu, R.J. Kee, J. Power Sources 117 (2003) 61–74.
[15] J. Larminie, A. Dicks, Fuel Cell Systems Explained, John Wiley & Sons Ltd., West Sussex, England, 2003.
[16] R.B. Bird, W.E. Stewart, E.N. Lightfoot, Transport Phenomenon, John Wiley & Sons Ltd., New York, 2002.
[17] E.A. Mason, A.P. Malinauskas, Gas Transport in Porous Media: The Dusty-Gas Model, Elsevier, New York, 1983.
[18] E.S. Greene, W.K.S. Chiu, M.G. Medeiros, J. Power Sources 161 (2006) 225–231.
[19] G. Ju, K. Reifsnider, X. Huang, Y. Du, J. Fuel Cell Sci. Technol. 1 (2004) 35–42.
[20] Y. Du, N.M. Sammes, J. Power Sources 136 (2004) 66–71.
[21] R.E. Williford, L.A. Chick, G.D. Maupin, S.P. Simner, J.W. Stevenson, J. Electrochem. Soc. 150 (2003) A1067–A1072.